ARTICLE

High Capacity and Excellent Stability of Lithium Ion Battery Anode Using Interface-Controlled Binder-Free Multiwall Carbon Nanotubes Grown on Copper

Indranil Lahiri,[†] Sung-Woo Oh,[‡] Jun Y. Hwang,[§] Sungjin Cho,[⊥] Yang-Kook Sun,[‡] Rajarshi Banerjee,[§] and Wonbong Choi*[,†,‡]

[†]Nano Materials and Device Lab, Department of Mechanical and Materials Engineering, Florida International University, Miami, Florida, [‡]Department of Energy Engineering, Hanyang University, Seoul, Korea, [§]Department of Materials Science and Engineering, University of North Texas, Denton, Texas, and [⊥]Material Research Lab, Marquette University, Milwaukee, Wisconsin

ABSTRACT We present a novel binder-free multiwall carbon nanotube (MWCNT) structure as an anode in Li ion batteries. The interface-controlled MWCNT structure, synthesized through a two-step process of catalyst deposition and chemical vapor deposition (CVD) and directly grown on a copper current collector, showed very high specific capacity, almost three times as that of graphite, excellent rate capability even at a charging/discharging rate of 3 C, and no capacity degradation up to 50 cycles. Significantly enhanced properties of this anode could be related to high Li ion intercalation on the carbon nanotube walls, strong bonding with the substrate, and excellent conductivity.

KEYWORDS: carbon nanotube · intercalation · lithium ion batteries · specific capacity · stability

High demand for rechargeable batteries in hybrid vehicles and portable electronic and medical devices have sparked research efforts in the development of lithium ion batteries with higher capacity and better stability in long-cycle operation.[1] Commercial Li ion batteries mostly use graphite as the anode material because of its excellent stability. However, because the theoretical specific capacity of graphite is low (372 mAh g^{-1}),[2] ample opportunity exists for the development of new anode materials with higher capacities. The introduction of nanomaterials as electrodes in the cells, in place of conventional electrodes, was intended to provide higher lithiation capability and an overall better performance simply because of the nanomaterials' extremely high surface area as compared to their bulk counterparts. Hence, much research effort was concentrated on selecting good (or the best) nanomaterials suitable for this application. Out of the many nanomaterials available, carbon nanotubes (CNTs) attracted much attention, mainly because of their excellent conductivity properties.[3] The application of CNTs in Li ion batteries dates back to 2001. However, all those initial efforts[4−6] could only obtain a maximum capacity of 280 mAh g^{-1}, much below the theoretical capacity of graphite. Though a few recent efforts have shown higher attainable reversible capacities using single-walled nanotubes (SWNTs), the processing techniques involve defect creation by etching or ball milling, use additives in electrolyte, and apply CNT paste (with organic binder) as anode.[7,8] However, like graphite, CNTs showed good stability in the long run.[9] Researchers also used other allotropes of carbon, graphene and fullerene and composites of them, as anodic replacement of graphite in Li ion cells.[10] The best capacity obtained from these materials is 784 mAh g^{-1} at a low current rate of 0.13 C (for graphene−fullerene composite), but with a capacity fading with cycles. Among other materials, Si and SnO_2 attracted much attention because of their very high theoretical specific capacities, 4200 and 782 mAh g^{-1}, respectively,[11,12] but both these materials suffer from the limitation that during Li ion intercalation and deintercalation, they experience huge (300−400%) expansion and contraction, resulting in pulverization and capacity loss in a high number of cycles. Though it was shown that an efficient design of their nanostructures can generate

*Address correspondence to choiw@fiu.edu.

Received for review February 26, 2010 and accepted April 28, 2010.

Published online May 4, 2010. 10.1021/nn100400r

very high capacity while minimizing the pulverization problem,[13,14] capacity degradation still occurred in long-cycle operation, though at a lower rate. In a different approach, nanocomposites of Si, SnO_2, other oxides (like CeO_2, CuO, *etc.*) and CNT/graphene were also used as the anode.[15−23] In spite of all such novel approaches, there exists ample opportunity for development of new anode structures for Li ion battery.

Commercial batteries and most of the research efforts have used polymeric binders in the anodes, adding a redundant weight, ultimately reducing the specific capacity of the electrode. Moreover, the most widely used binder, poly(vinylidene fluoride) (PVdF), is known to react with graphitic materials and metallic lithium to form stable compounds.[24−27] Such reactions are highly exothermic; for example, the reaction with metallic Li produces 7.2 kJ of energy per gram of PVdF.[24] Thus, the presence of a binder could lead to thermal runaway, necessitating incorporation of additional safety features in the battery. Advanced Li ion batteries, hence, need a binder-free electrode, to avoid such a type of capacity loss and which will include additional safety features. To address all these issues, we propose here direct synthesis of interface-controlled multiwall carbon nanotubes (MWCNTs) on copper current collectors and their application as the anode in Li ion cells. This kind of structure is expected to have many advantages over the conventional anodes. First of all, unlike all the past studies involving CNTs, which used raw CNTs and polymeric binders,[4−6] the present structure has directly grown CNTs on the current collector, thus avoiding the polymeric binders completely. In this way, it reduces harmful effect of the polymeric binder, reduces weight of the active material, increases specific capacity, and shows potential to be used for high temperature application. Second, CNTs do not have any kind of expansion/contraction and pulverization problem (like Si and SnO_2), so they can sustain their capacity for long cycles. Third, due to growth, each CNT is well bonded to the current collector, thus all of them contribute to the capacity. Fourth, the high specific surface area of CNTs allows more Li ion intercalation. Fifth, higher conductivity of the active anode material is important for achieving higher capacity.[28] In that respect, MWCNTs, known to be excellent charge carriers, are an alternative option and aid in achieving higher capacity. Moreover, by the interface-control, proposed in this study, an ohmic contact and strong bonding between the CNTs and substrate are ensured, which further helps in efficient charge transport. Further, the anode structure, consisting of MWCNTs grown on Cu foil, can be very easily fabricated using the thermal chemical vapor deposition (CVD) process (see Materials and Methods section).[29]

RESULTS AND DISCUSSION

The novel anode structure was prepared by depositing catalysts by sputtering onto Cu foils, followed by MWCNT growth by CVD. Electrochemical studies were performed on half cells prepared by CR2032 press. Electrochemical characteristics of the MWCNT-on-Cu electrode are presented in Figure 1. First two charge−discharge curves, at a current rate of 0.1 C (38 mAg^{-1}, assuming theoretical specific capacity same as that of graphite, *i.e.,* 372 mAh g^{-1}), are shown in Figure 1a. The first discharge cycle is characterized by very high capacity (>2500 mAh g^{-1}) and a plateau in the voltage region 0.9−0.5 V. Such plateau is typical of all CNT-based electrodes and is related to decomposition of the electrolyte and formation of solid electrolyte interphase (SEI) on the CNT surface.[30] The plateau was not observed from the next cycle onward, indicating that SEI formation was complete in the first discharge cycle itself. The first charge cycle showed a capacity of 1455 mAh g^{-1} and hence, an irreversible capacity loss of 42%. However, the second discharge and charge cycles almost maintained the reversible capacity from the first cycle. A good portion of capacity was found to be at a voltage range greater than 0.5 V, which is a common feature for any kind of nanostructured carbon anode materials and even for C−Si core−shell nanowires.[10,12,31,32] Though this type of behavior is different from that shown by graphite electrodes,[33] it does not affect the full-cell characteristics much, as was shown in the case of the C−Si core−shell nanowire structure.[32]

The rate capability of the electrode is shown in Figure 1b. The reversible capacity of the electrode was found to be very high and quite stable (especially, after few initial cycles). Even at a very high charging/discharging rate of 3.0 C (1.116 Ag^{-1}), the electrode showed a reversible capacity of 767 mAh g^{-1}, representing 106% increment in capacity as compared to the theoretical capacity of graphite anodes. To specifically understand the stability of the capacity, the electrode was subjected to 50 charge/discharge cycles at 1.0 C rate (372 mAg^{-1}), after two initial cycles each at 0.1 C and 0.5 C (186 mA g^{-1}) rates (Figure 1c). The figure shows a very high capacity of the electrode (∼900 mAh g^{-1}, 140% enhancement as compared to theoretical capacity of graphite) at this rate and excellent stability of the capacity over 50 cycles. In fact, there was no capacity degradation during these 50 cycles (except for the initial two cycles). The Coulombic efficiency of the electrode was also very high, more than 99%, after two initial cycles at 1.0 C rate (Figure 1d). Such high capacity and nil capacity degradation over 50 cycles make this electrode a suitable alternative to the graphite anodes conventionally used in Li ion batteries. Apart from its high-cycle stability, the interface-controlled MWCNT-on-Cu anode has shown higher capacity than any other anode fabricated by carbon nano/meso-structure and

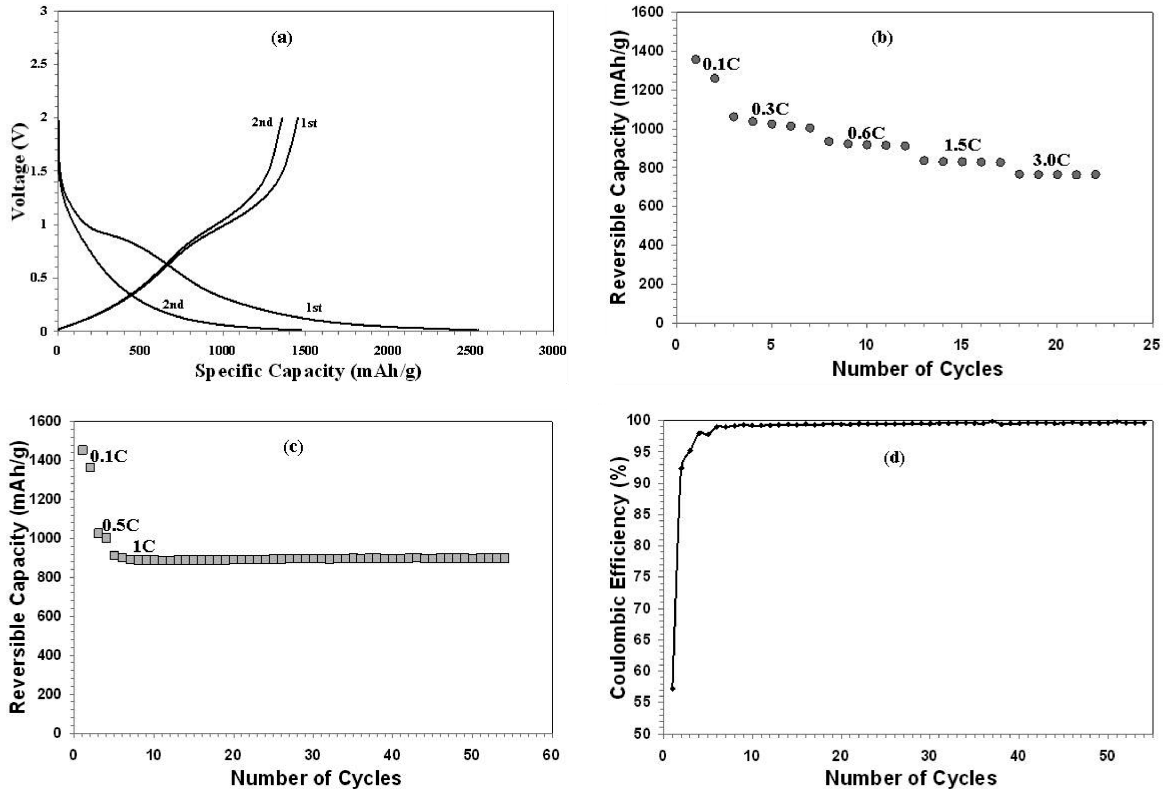

Figure 1. Electrochemical characteristics of the proposed CNT-based electrode structure. (a) First two charge−discharge cycles of the MWNT-on-Cu anode, at 0.1 C rate. The first discharge cycle (lithiation) has shown a very high capacity of 2547 mAh g^{-1}, while the following delithiation cycle showed a specific capacity of 1455 mAh g^{-1}. (b) Reversible capacity of the MWNT-on-Cu anode, at different C-rates. Very high specific capacity could be observed at all C-rates. Even at the 3 C rate, a reversible capacity of 767 mAh g^{-1} was observed, which is almost 2 times the theoretical capacity of graphite. (c) Exceptional stability of the reversible capacity (~900 mAh g^{-1}) of the MWNT-on-Cu anode in long-run, at 1 C rate. Except for the first two cycles, virtually no capacity degradation was observed for this anode structure, in 50 cycles. (d) Coulombic efficiency of the MWNT-on-Cu anode, showing very high efficiency, except for the first cycle. After the initial five cycles, the efficiency remained more than 99%.

its composites, at all the current rates (see Supporting Information, Figure 1).

It is well understood that the unique structure of the proposed anode is responsible for its excellent performance. To better understand the structure and lithiation−delithiation mechanism, a thorough structural characterization, using SEM, high resolution transmission electron microscope (HRTEM), X-ray diffraction, and Raman spectroscopic analysis has been performed (see Figure 2 and Supporting Information). X-ray diffraction (see Supporting Information, Figure 2) and Raman spectroscopy analysis (Figure 2d) show an increase in defect density in the CNTs in the lithiated state, as compared to the as-grown state, followed by a lesser defect density in the delithiated condition. Figure 2a (and its inset) shows an SEM micrograph of the as-grown CNTs on the Cu current collector, while Figure 2b (and its inset) shows TEM micrographs of the same structure. The CNTs (outer diameter ≈ 100 nm), which form a forest-like structure of ~30 μm height on the Cu current collector, allow formation of a porous structure that opens up a huge surface area of CNTs, thus increasing the lithiation capability of the electrode. The as-grown CNTs also show some amount of defects in the structure (inset of Figure 2b), which can probably lead to enhanced Li ion intercalation. Some of the CNTs are found to be twisted (Figure 2c). The twisting increases the specific surface area of CNTs, which is probably one of the reasons for high Li insertion in these CNTs. No noticeable volume expansion of the CNTs was observed after lithiation. Figure 2b,e and f shows representative SEM micrograpghs of CNTs in as-grown, lithiated, and delithiated states respectively, indicating that the diameter of CNTs remained almost constant (~100 nm). This observation is unique and distinctly different from the observations made by Maurin *et al.*, who has reported swelling and shrinkage of CNTs, during the lithiation and delithiation.[34]

A quick comparison of the structure of the CNTs, in the lithiated and the delithiated states can be performed from the TEM images in Figure 2, panels e−h. The lithiated CNT structures clearly show formation of a thick layer of a second phase (the lithiated phase) on their walls, while such a second phase structure could not be observed in the delithiated condition. To minimize exposure of the sample to air, the sample preparation was carried out in Ar glovebox. In a separate study (see Supporting Information, Figure 4), the effect of

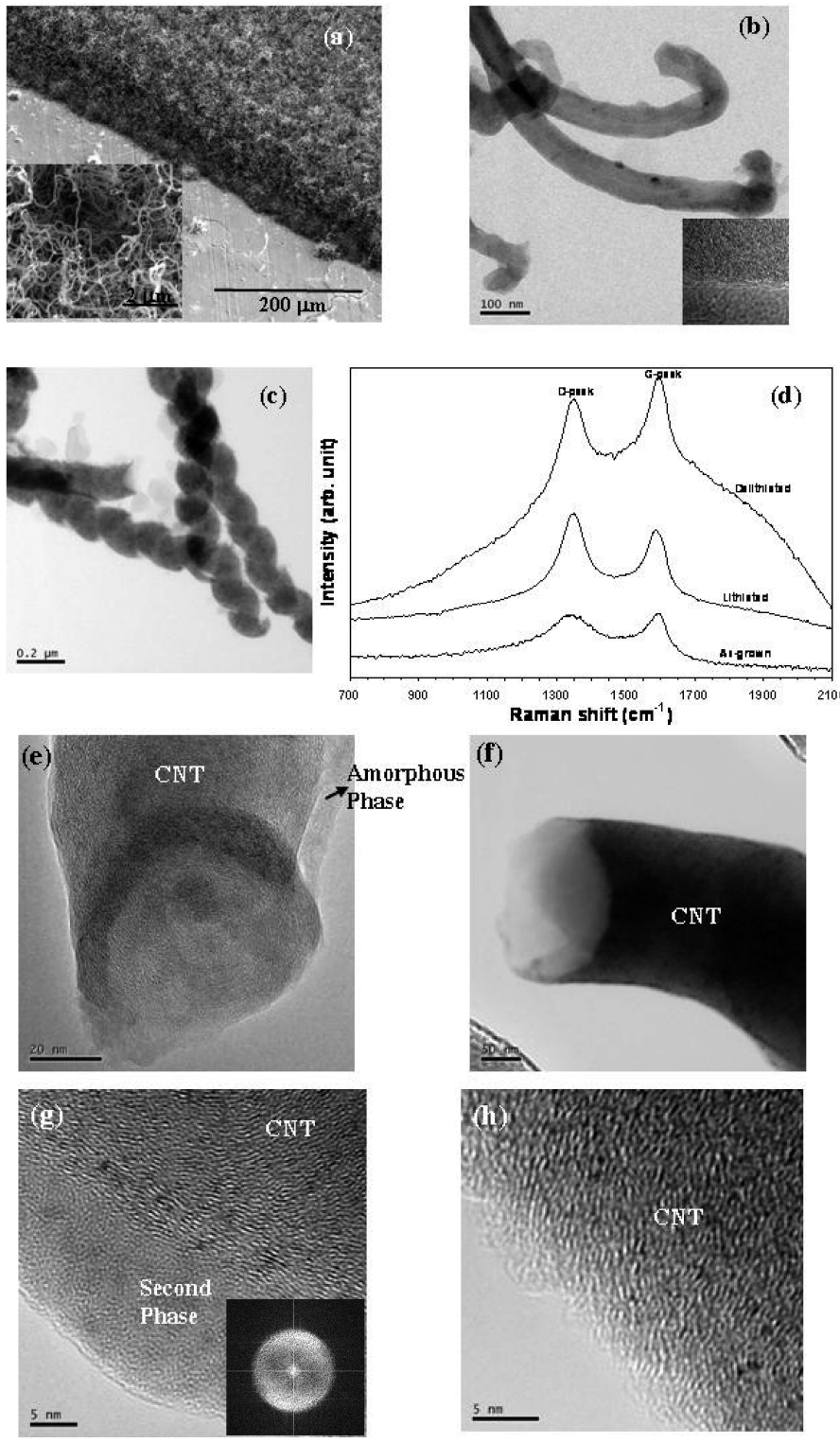

Figure 2. Structure of the electrode in as-grown, lithiated, and delithiated states. (a) SEM and (b) TEM images of the as-grown MWNT-on-Cu structure (insets are at higher magnification), showing a forest-like structure of randomly oriented CNTs (individual MWNTs are around 100 nm thick) on the Cu current collector, allowing formation of a porous structure and opening up a huge surface area of CNTs, thus increasing the lithiation capability of the electrode. The as-grown CNTs also show some amount of defects in the structure (inset of Figure 2b), which can probably lead to enhanced Li ion intercalation. Panel c shows the presence of twisting in the as-grown sample, which also increases surface area of CNTs. (d) Comparison of Raman spectroscopic response from the CNTs in different conditions. I_D/I_G ratio in Raman spectra, which indicates purity or crystallinity of CNTs, increases from 0.95 for the pristine sample to 1.21 in the lithiated condition and decreases to 0.94 in the delithiated condition. So, the crystallinity of the CNTs is lost in the lithiated state and recovers in the delithiation stage. (e, g) TEM images of the CNTs in the lithiated condition, showing formation of Li−C phase at the walls (FFT image at inset) and loss of crystallinity at those positions. (f, h) TEM images of the CNTs in the delithiated condition, showing the absence of the second phase and partial recovery of the crystallinity at the walls.

long-time air exposure on the structure has been shown to form Li_2O, a visibly different structure. Hence, the thick layer on the lithiated CNTs is expected to be an amorphous lithiated carbon phase only. The formation of such structures was found throughout the whole lithiated sample. This amorphous lithiated phase is expected to have a stoichiometry of LiC_x, ($x = 2-6$), as reported previously for C-based anodes of Li ion batteries.[35] Though the specific stoichiometry of the lithiated compound is not known, the very high defect density of CNTs and high reversible capacity (>900 mAh g^{-1}), which is comparable to the theoretical capacity (1116 mAh g^{-1}) of SWCNTs (forming LiC_2),[8,35] indicate that the composition is likely to be LiC_x ($x = 2-3$). However, the composition needs to be confirmed by the Li NMR technique. These results clearly indicate that during lithiation CNTs partly lose their crystallinity along the outer surface, probably due to their interaction with the Li^+ ions. However, the same samples in the delithiated state do not show the presence of the thick amorphous phase on the walls of the CNTs (see Figure 2f,h). It is not very clear if the loss of crystallinity is fully recovered during the delithiation process, but the HRTEM images of the delithiated sample exhibit better crystallinity, demonstrating at least a partial recovery of the loss of crystallinity.

Structural characterization of the samples, in different stages of lithiation, sheds light on the mechanism of lithium insertion and extraction into the anode and highlights the advantages of the anode structure. An initial higher defect density of the pristine CNTs, as evident from the Raman spectroscopic analysis, XRD, and HRTEM, might have helped the anode structure to show very high capacity, as a defective CNT structure is known to have a higher conductivity than graphitic CNTs[36] and better lithiation capability.[31] Moreover, twisted CNTs offer higher specific surface area and hence probably more Li ion intercalation. During lithiation, Li^+ ions reach individual CNTs, passing easily through the CNT forest structure, and attach with their sidewalls. A very high surface area of the CNTs promotes a huge amount of Li^+ ion intercalation. On the other hand, during delithiation, most of the ions return back to the opposite electrode. The highly porous nature of the CNT forest structure allows easy transport of the intercalating ions from one electrode to the other. A schematic of the lithiation−delithiation mechanism is given in Figure 3c.

It is very important for the Li ion battery to have an efficient electron transport from the current collectors to the *CNTs* to show good cycling behavior. Our interface-controlled MWCNT structure, grown directly on the Cu current collector, ensures minimum resistance. Through our choice of diffusion barrier layer and catalyst layer (Ti and Ni, respectively), we have minimized the presence of high-resistivity material in the electron path. Total resistance of the electrode structure (Cu to CNT tip), as measured by a two-probe method, is found to be 3.3 Ω, which is considered to be very low. It may be mentioned here that such contact resistance measurements between the substrate and CNT tip resulted in a lowest value of ~135 Ω,[37] which is almost 40 times higher than the values found in the present study. One of the reasons for achieving such low contact resistance is the presence of Ti, which is known to show very low (an order of magnitude lower than that of Pd, Pt, Cu, and Au) contact resistance with CNTs.[38] Moreover, it is necessary to have good bonding between the substrate and the CNTs in order to avoid pulverization and to achieve good stability at a high-cycle. To investigate more into the Cu−CNT interface, HRTEM images, taken from the interface region of the pristine sample, were studied

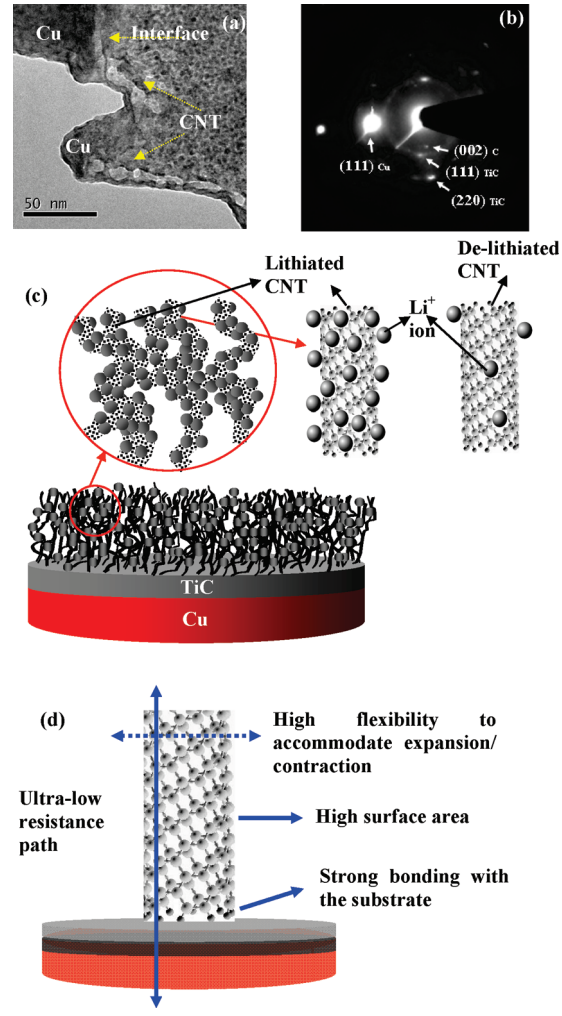

Figure 3. Structural analysis of the proposed anode. (a) HRTEM image of substrate−CNT interface, showing a well-bonded interface and the presence of an interfacial phase. The selective area diffraction pattern (b) shows formation of TiC at the interface, which also helped in making the bonding strong and conductive. (c) A schematic (not to scale) of the proposed lithiation−delithiation mechanism, showing a huge amount of Li^+ ion intercalated to the walls of the CNTs during lithiation and deintercalation of most of the ions in delithiation. (d) A schematic (not to scale) of the proposed anode structure, showing its advantageous features.

(Figure 3a,b). The HRTEM image shows very good bonding between the substrate and the CNT layer, through formation of an interface layer. A selective area diffraction pattern (SADP) taken from this interface region shows the presence of TiC. Formation of TiC, in the interface, helps in two ways: first, TiC, being highly conductive, provides low-resistance paths for electron movement from the Cu current collector to the CNTs, and, second, it ensures a strong bond formation between the substrate and the CNT.[39]

The benefits of using an interface-controlled MWCNT structure, directly grown on a Cu current collector, as the anode material in Li ion batteries can be understood from the schematic presented in Figure 3d. As shown in the drawing, this proposed structure offers many advantages: (i) CNT structure does not show any expansion/contraction problem during lithiation/delithiation and hence pose no threat of pulverization; (ii) a very high surface area of CNTs is available for lithiation and easy ion transport through the highly porous CNT forest structure; (iii) formation of TiC allows a strong bonding of the CNTs with the substrate, thus minimizing breakage and improving the long-cycle behavior, and (iv) from CNT tip to copper current collector, the structure presents an ultralow resistance path (CNTs having the highest current carrying capacity, $\sim 10^9$ A/cm^2 and substrate material also being highly conductive), which aids in faster charge transport. All these beneficial factors of the interface-controlled MWCNT structure on the copper current collector aid in enhancement of the capacity of the electrode and provide excellent stability. The stability offered by our MWCNT-based electrode shows comparable performance with Si nanostructure-based electrodes[40,41] and an even better capacity of 900 mAh g^{-1} at a current rate of 1 C as compared to that of a C−Si core−shell nanowire (Figure 3d of ref 32).

In the present study, we have developed a novel MWCNT-based binder-free anode structure, through a simple two-step process, which shows good specific capacity, even at high current rate of 3 C and excellent stability (nil capacity degradation) over 50 cycles. While better safety is expected from the binder-free nature of the electrodes, interface-controlled growth of CNTs on Cu current collectors ensures good bonding and excellent conductivity. Our MWCNT-based anode is anticipated to be one of the best suitable materials for future Li ion battery anodes.

MATERIALS AND METHODS

Preparation of the Electrode Structure. A 50 μm thick pure copper foil (Fischer Scientific, 99.9% purity) was punched to 14 mm diameter and used as substrates for depositing thin films of Ti and Ni (thickness 20−25 nm) through a RF magnetron sputtering system (AJA International). These coated samples were then inserted into a thermal chemical vapor deposition (CVD) system for direct CNT growth. During the initial stage of CVD, the sample was heated very fast, under an Ar gas envelope, to the growth temperature range of 973−1173 K, and the CNT growth started with introduction of a $H_2 + C_2H_4$ gas mixture (1:2 ratio) in the chamber as the precursor. At the end of the growth period, samples were slowly cooled to room temperature within the furnace, under an inert (Ar) gas envelope. Samples were weighed before and after CVD growth to calculate the weight of CNTs.

Structural Characterization. The morphology of the electrode structure was analyzed in a field emission SEM (JEOL, JSM7000F) and Raman spectrometer (Ar^+ laser with $\lambda = 514$ nm, 15 mW power). The electrode structures were also characterized by X-ray diffraction (Rigaku, Rint-2000), using Cu Kα radiation, in the range of 10−120° (2θ), with a step size of 0.03°. The CNT structure and the interface between the Cu substrate and CNTs were characterized using FEI TECHNAI F20 field emission TEM, operating at 200 kV. A site specific sample was prepared for the HRTEM study, using FEI Nova 200 NanoLab dual-beam FIB. Details about HRTEM sample preparation is available in ref 42.

Electrochemical Characterization. Electrochemical behavior of the structure, as a proposed anodic material in Li ion batteries, has been studied in a typical coin cell (half-cell). The coin cells were prepared in a CR2032 press (Hohsen Corp., Japan). The complete cell preparation steps were performed in an argon glovebox (Unilab Mbrann), maintaining the oxygen and humidity level (both individually <0.1 ppm) within the chamber. A pure Li (purity, 99.9%) metal foil (150 μm thick) was used as the reference electrode and counter-electrode, while the MWCNT-on-Cu was used as the working electrode. All the coin cells used 1.0 M $LiPF_6$ in EC-DEC (1:1 in volume) (ethylene carbonate−diethyl carbonate) as the electrolyte, and a typical polypropylene−polyethylene material (Celgard 3401) as the separator.

The charge−discharge behavior of the coin cells were characterized in TOSCAT 3100U multichannel battery testing unit, at a constant temperature of 30 °C, in galvanostatic mode. The instrument was programmed to read in each 10 mV step. The cells were cycled in the voltage range 2.0−0.01 V, at a very slow rate (0.1 C), during the initial formation process and at different rates in the following cycles.

Acknowledgment. I. Lahiri and W. Choi thank Dr. K. W. Jones, Director, AMERI, FIU, Mr. Neal Ricks, Manager, Nano-fabrication facility, AMERI, FIU, and Dr. S. Saxena, Director, CeSMEC, FIU, for allowing to use of their research facilities. This research was, in part, supported by WCU (World Class University) program through the Korea Science and Engineering Foundation funded by the Ministry of Education, Science and Technology (R31-2008-000-10092).

Supporting Information Available: XRD plot, additional TEM images, and capacity comparison with other anode materials. This material is available free of charge *via* the Internet at http://pubs.acs.org.

REFERENCES AND NOTES

1. Nazri, G.-A.; Pistoia, G. In *Lithium Batteries: Science and Technology*; Springer Science+Business Media: New York, 2009.
2. Manev, V.; Naidenov, I.; Puresheva, B.; Zlatilova, P.; Pistoia, G. Electrochemical Performance of Natural Brazilian Graphite as Anode Material for Lithium-Ion Rechargeable Cells. *J. Power Sources* **1995**, *55*, 211–215.
3. Dai, H.; Javey, A.; Pop, E.; Mann, D.; Lu, Y. Electrical Transport Properties and Field Effect Transistors of Carbon Nanotubes. *Nano* **2006**, *1*, 1–13.
4. Yang, Z.-H.; Wu, H.-Q. Electrochemical Intercalation of Lithium into Raw Carbon Nanotubes. *Mater. Chem. Phys.* **2001**, *71*, 7–11.

5. Frackowiak, E.; Béguin, F. Electrochemical Storage of Energy in Carbon Nanotubes and Nanostructured Carbons. *Carbon* **2002**, *40*, 1775–1787.
6. Shin, H.-C.; Liu, M.; Sadanadan, B.; Rao, A. M. Electrochemical Insertion of Lithium into Multiwalled Carbon Nanotubes Prepared by Catalytic Decomposition. *J. Power Sources* **2002**, *112*, 216–221.
7. Eom, J. Y.; Kwon, H. S. Improved Lithium Insertion/Extraction Properties of Single-Walled Carbon Nanotubes by High-Energy Ball Milling. *J. Mater. Res.* **2008**, *23*, 2458–2466.
8. Landi, B. J.; Ganter, M. J.; Schauerman, C. M.; Cress, C. D.; Raffaelle, R. P. Lithium Ion Capacity of Single Wall Carbon Nanotube Paper Electrodes. *J. Phys. Chem. C* **2008**, *112*, 7509–7515.
9. Guo, A. P.; Zhao, Z. W.; Liu, H. K.; Dou, S. X. Electrochemical Lithiation and Delithiation of MWNT-Sn/SnNi Nanocomposites. *Carbon* **2005**, *43*, 1392–1399.
10. Yoo, E. J.; Kim, J.; Hosono, E.; Zhoi, H.-S.; Kudo, T.; Honma, I. Large Reversible Li Storage of Graphene Nanosheet Families for Use in Rechargeable Lithium Ion Batteries. *Nano Lett.* **2008**, *8*, 2277–2282.
11. Boukamp, B. A.; Lesh, G. C.; Huggins, R. A. All-Solid Lithium Electrodes with Mixed-Conductor Matrix. *J. Electrochem. Soc.* **1981**, *128*, 725–729.
12. Paek, S.-M.; Yoo, E.-J.; Honma, I. Enhanced Cyclic Performance and Lithium Storage Capacity of SnO_2/Graphene Nanoporous Electrodes with Three-Dimensionally Delaminated Flexible Structure. *Nano Lett.* **2009**, *9*, 72–75.
13. Fan, J.; Wang, T.; Yu, C.; Tu, B.; Jiang, Z.; Zhao, D. Ordered, Nanostructured Tin-Based Oxides/Carbon Composite as the Negative-Electrode Material for Lithium-Ion Batteries. *Adv. Mater.* **2004**, *16*, 1432–1436.
14. Chan, C. K.; Peng, H.; Liu, G.; McIlwrath, K.; Zhang, X. F.; Huggins, R. A.; Cui, Y. High-Performance Lithium Battery Anodes Using Silicon Nanowires. *Nat. Nanotechnol.* **2008**, *3*, 31–35.
15. Shu, J.; Li, H.; Yang, R.; Shi, Y.; Huang, X. Cage-like Carbon Nanotubes/Si Composite as Anode Material for Lithium Ion Batteries. *Electrochem. Commun.* **2006**, *8*, 51–54.
16. Wang, Y.; Zeng, H. C.; Lee, J. Y. Highly Reversible Lithium Storage in Porous SnO_2 Nanotubes with Coaxially Grown Carbon Nanotube Overlayers. *Adv. Mater.* **2006**, *18*, 645–649.
17. Zhang, Y.; Zhang, X. G.; Zhang, H. L.; Zhao, Z. G.; Li, F.; Liu, C.; Cheng, H. M. Composite Anode Material of Silicon/Graphite/Carbon Nanotubes for Li ion Batteries. *Electrochim. Acta* **2006**, *51*, 4994–5000.
18. Eom, J. Y.; Park, J. W.; kwon, H. S.; Rajendran, S. Electrochemical Insertion of Lithium into Multiwall Carbon Nanotube/Silicon Composites Produced by Ball Milling. *J. Electrochem. Soc.* **2006**, *153*, A1678–A1684.
19. Wang, W.; Kumta, P. N. Reversible High Capacity Nanocomposite Anodes of Si/C/SWNTs for Rechargeable Li ion Batteries. *J. Power Sources* **2007**, *172*, 650–658.
20. Park, M.-S.; Needham, S. A.; Wang, G.-X.; Kang, Y.-M.; Park, J.-S.; Dou, S.-X.; Liu, H.-K. Nanostructured SnSb/Carbon Nanotube Composites Synthesized by Reductive Precipitation for Lithium-Ion Batteries. *Chem. Mater.* **2007**, *19*, 2406–2410.
21. Li, C.; Sun, N.; Ni, J.; Wang, J.; Chu, H.; Zhou, H.; Li, M.; Li, Y. Controllable Preparation and Properties of Composite Materials Based on Ceria Nanoparticles and Carbon Nanotubes. *J. Solid State Chem.* **2008**, *181*, 2620–2625.
22. Chen, G.; Wang, Z.; Xia, D. One-Pot Synthesis of Carbon Nanotube@SnO_2-Au Coaxial Nanocable for Lithium-Ion Batteries with High Rate Capability. *Chem. Mater.* **2008**, *20*, 6951–6956.
23. Zheng, S.-F.; Hu, J.-S.; Zhong, L.-S.; Song, W.-G.; Wan, L.-J.; Guo, Y.-G. Introducing Dual Functional CNT Networks into CuO Nano/Micro Spheres toward Superior Electrode Materials for Lithium-Ion Batteries. *Chem. Mater.* **2008**, *20*, 3617–3622.
24. Zhang, S. S.; Jow, T. R. Study of Poly(Acrylonitrile-Methyl Methacrylate) as Binder for Graphite Anode and $LiMn_2O_4$ Cathode of Li ion Batteries. *J. Power Sources* **2002**, *109*, 422–426.
25. Guerfi, A.; Kaneko, M.; Petitclerc, M.; Mori, M.; Zaghib, K. $LiFePO_4$ Water-Soluble Binder Electrode for Li ion Batteries. *J. Power Sources* **2007**, *163*, 1047–1052.
26. Zhang, S. S.; Xu, K.; Jow, T. R. Evaluation on a Water-Based Binder for the Graphite Anode of Li ion Batteries. *J. Power Sources* **2004**, *138*, 226–231.
27. Roth, E. P.; Doughty, D. H.; Franklin, J. DSC Investigation of Exothermic Reactions Occurring at Elevated Temperatures in Lithium-Ion Anodes Containing PVDF-Based Binders. *J. Power Sources* **2004**, *134*, 222–234.
28. Ishihara, T.; Nakasu, M.; Yoshio, M.; Nishiguchi, H.; Takita, Y. Carbon Nanotube Coating Silicon Doped with Cr as a High Capacity Anode. *J. Power Sources* **2005**, *146*, 161–165.
29. Choi, W. B.; Cho, S. J.; Lahiri, I. *High Efficiency Lithium Ion Battery Anode Using Interface-Controlled Binder-Free Carbon Nanotubes Grown on Metal/Alloy Substrates*. U.S. Patent Appl. No. 61/222,481 (Filing date: 07/02/2009).
30. Chen, W. X.; Lee, J. Y.; Liu, Z. Electrochemical Lithiation and Delithiation of Carbon Nanotube−Sn_2Sb Nanocomposites. *Electrochem. Commun.* **2002**, *4*, 260–265.
31. Masarapu, C.; Subramanian, V.; Zhu, H.; Wei, B. Long-Cycle Electrochemical Behavior of Multiwall Carbon Nanotubes Synthesized on Stainless Steel in Li ion Batteries. *Adv. Funct. Mater.* **2009**, *19*, 1008–1014.
32. Cui, L.-F.; Yang, Y.; Hsu, C.-M.; Cui, Y. Carbon−Silicon Core−Shell Nanowires as High Capacity Electrode for Lithium Ion Batteries. *Nano Lett.* **2009**, *9*, 3370–3374.
33. Kakshedikar, N. A.; Maier, J. Lithium Storage in Carbon Nanostructures. *Adv. Mater.* **2009**, *21*, 2664–2680.
34. Maurin, G.; Bousquet, Ch.; Henn, F.; Bernier, P.; Almairac, R.; Simon, B. Electrochemical Intercalation of Lithium into Multiwall Carbon Nanotubes. *Chem. Phys. Lett.* **1999**, *312*, 14–18.
35. Nishidate, K.; Hasegawa, M. Energetics of Lithium Ion Adsorption on Defective Carbon Nanotubes. *Phys. Rev. B* **2005**, *71*, 245418.
36. Watts, P. C. P.; Hsu, W.-K.; Kroto, H. W.; Walton, D. R. M. Are Bulk Defective Carbon Nanotubes Less Electrically Conducting. *Nano Lett.* **2003**, *3*, 549–553.
37. Parthangal, P. M.; Cavicchi, R. E.; Zachariah, M. R. A Generic Process of Growing Aligned Carbon Nanotubes Arrays on Metals and Metal Alloys. *Nanotechnology* **2007**, *18*, 185605−1-5.
38. Matsuda, Y.; Deng, W.-Q.; Goddard, W. A. III. Contact Resistance Properties between Nanotubes and Various Metals from Quantum Mechanics. *J. Phys. Chem. C* **2007**, *111*, 11113–11116.
39. Zhang, J.; Wang, X.; Yang, W.; Yu, W.; Feng, T.; Li, Q.; Liu, X.; Yang, C. Interaction between Carbon Nanotubes and Substrate and its Implication in Field Emission Mechanism. *Carbon* **2006**, *44*, 418–422.
40. Huang, R.; Fan, X.; Shen, W.; Zhu, J. Carbon-Coated Silicon Nanowire Array Films for High-Performance Lithium-Ion Battery Anodes. *Appl. Phys. Lett.* **2009**, *95*, 133119.
41. Park, M.-H.; Kim, M. G.; Joo, J.; Kim, K.; Kim, J.; Ahn, S.; Cui, Y.; Cho, J. Silicon Nanotube Battery Anodes. *Nano Lett.* **2009**, *9*, 3844–3847.
42. Lahiri, I.; Seelaboyina, R.; Hwang, J. Y.; Banerjee, R; Choi, W. Enhanced Field Emission from Multiwalled Carbon Nanotubes Grown on Pure Copper Substrate. *Carbon* **2010**, *48*, 1531–1538.